JOURNAL OF GEOPHYSICAL RESEARCH, VOL. 102, NO. D4, PAGES 4475–4486, FEBRUARY 27, 1997

Aliased power of a stochastic temperature field on a sphere

Ta-Hsin Li
Department of Statistics, Texas A&M University, College Station

Gerald R. North
Climate System Research Program, Department of Meteorology, Texas A&M University, College Station

Samuel S. Shen[1]
Center for Climate System Research, University of Tokyo, Tokyo, Japan

Abstract. A random climate field over the globe can be decomposed into a series of spherical harmonic functions. This paper shows that the mean square sampling error for a spherical harmonic coefficient is composed of aliased powers from other spherical harmonic components due to the spatial gaps in sampling networks. A general formula is given for calculating the aliased powers. On the basis of the spectra derived from a noise-forced linear energy balance model (EBM) for the climate field the aliased powers are investigated in detail for the Gauss-Legendre networks and the latitude-longitude uniform networks. It is found that the Gauss-Legendre networks outperform the uniform networks of the same size as long as the number of stations is sufficiently large.

1. Introduction

There are many instances in climatology in which the spherical harmonic basis set is advantageous. For example, many general circulation models (GCMs) employ them as part of their numerical scheme (the so-called pseudo-spectral methods). The spherical harmonics also form a convenient basis set for archiving data. Truncating such an expansion leads to the natural interpretation of excluding scales smaller than a preset length on the sphere. There arises the problem of estimating the coefficients in the expansion from imperfect observing systems. In this paper we consider the observing system to be a given set of discrete points on the sphere—observing stations. We are interested in the random errors due to a lack of sufficient density of the stations and the systematic errors due to aliasing—the tendency for error in unresolved scales to contaminate the estimate in resolved scales. In particular, we are interested in estimating the coefficients for a particular temporal snapshot or for a time average of an evolving field. We are given the values of the field at a set of points on the sphere, and we wish to estimate the spherical harmonic coefficients from these measurements. In our examples we employ a stochastic climate model in its low-frequency limit. In this simple model the geography of the land-sea distribution drops out, and the statistics of the random temperature field become homogeneous on the sphere. This simplification allows for analytical results, but in principle, a nonhomogeneous field could also be treated by the described methodology.

In this paper we take the field to have some special symmetries for convenience, but we intend in later studies to generalize the findings to less symmetrical situations. We shall also take our sets of points to have some special symmetry properties to make the computations more transparent. In particular, we pay special attention to the Gauss-Legendre (GL) design (section 3) which has been utilized in many spectral GCMs. This grid is the one in which the points are equally spaced along latitude circles but located at the zeros of the Legendre polynomials in latitude along the meridians. With the GL design one is able to achieve an aliasing-free transformation between the spectral domain and the physical domain for band-limited fields [*Washington and Parkinson*, 1986; *Chen*, 1993; *Li and North*, 1996]. In section 4 of this paper we evaluate the aliased power of the GL design for the climate fields that may not be band limited. In particular, we present some numerical examples in section 6 based on a white noise driven EBM (section 5) whose power spectrum is not band limited but decays rapidly with respect to the wave numbers. Under this climate model we compare

[1]Now at Department of Mathematical Sciences, University of Alberta, Edmonton, Canada.

Paper number 96JD03376.
0148-0227/97/96JD-03376$09.00

the aliased power of the GL design with that of the latitude-longitude uniform (LLU) design in which the grid points are uniformly spaced along both latitude and longitude circles. The comparison shows that the GL design eventually outperforms the LLU design if the number of sampling points is sufficiently large. Concluding remarks are given in section 7.

2. Concept of Sampling Design

We regard the Earth as a perfect sphere of unit radius. Therefore locations on the Earth are determined by the unit vector $\boldsymbol{n} = (\cos\phi\cos\theta, \cos\phi\sin\theta, \sin\phi)$ that points to the location in question from the center of the sphere, with latitude $\phi \in (-\pi/2, \pi/2]$ and longitude $\theta \in (-\pi, \pi]$. Let $T(\boldsymbol{n})$ denote the surface air temperature field, which is random in nature. Then the spherical random field $T(\boldsymbol{n})$ can be expanded into a series of spherical harmonics $Y_{lm}(\boldsymbol{n})$, so that

$$T(\boldsymbol{n}) = \sum_{l=0}^{\infty} \sum_{m=-l}^{l} T_{lm} Y_{lm}(\boldsymbol{n}), \tag{1}$$

where l represents the meridional wave number (or degree) and m represents the zonal wave number. The spherical harmonic coefficients T_{lm} in (1) are determined by

$$T_{lm} = \int T(\boldsymbol{n})\, Y^*_{lm}(\boldsymbol{n})\, d\Omega, \tag{2}$$

where $Y^*_{lm}(\boldsymbol{n})$ is the complex conjugate of $Y_{lm}(\boldsymbol{n})$ and the integration is over the unit sphere. Strictly speaking, the expansion (1) is subject to certain conditions that must be satisfied by $T(\boldsymbol{n})$. But we are not going to dwell on these conditions. Interested readers are referred to the paper by *Li and North* [1996].

Suppose the surface air temperature field $T(\boldsymbol{n})$ is observed from J stations located at $\{\boldsymbol{n}_1, \cdots, \boldsymbol{n}_J\}$. We use the observed data $\{T(\boldsymbol{n}_j)\}_{j=1}^J$ to estimate the spherical harmonic coefficients T_{lm} defined by (2). Simple linear estimators of T_{lm} take the form

$$\hat{T}_{lm} = \sum_{j=1}^{J} w_j\, T(\boldsymbol{n}_j)\, Y^*_{lm}(\boldsymbol{n}_j), \tag{3}$$

where the w_j are real-valued weights satisfying the normalization condition

$$\sum_{j=1}^{J} w_j = 4\pi. \tag{4}$$

Let $\boldsymbol{n}_j = (\cos\phi_j\cos\theta_j, \cos\phi_j\sin\theta_j, \sin\phi_j)$. Then the sampling design, in general, requires one to choose the $3J$ real-valued parameters $\{\phi_1, \cdots, \phi_J\}$, $\{\theta_1, \cdots, \theta_J\}$, and $\{w_1, \cdots, w_J\}$ in the estimator (3) under a certain optimization criterion. Because of the constraint in (4) the number of free parameters to be chosen equals $3J-1$. Note that one may also choose different weights for different spherical harmonic coefficients, so that $w_j = w_j^{(lm)}$ depends on the wave numbers l and m. In this paper, however, we restrict ourselves to the case in which the weights are wave number independent.

2.1. Partially Aliasing Free Sampling

There are many ways of designing a sampling network [*Hardin and Upson*, 1993; *Shen et al.*, 1994; *Kim et al.*, 1996]. In this paper we consider a design that forces the aliasing-free identity

$$\hat{T}_{lm} = T_{lm} \tag{5}$$

to hold for as many wave numbers l and m as possible. This idea is similar to that of the Gaussian quadrature in numerical analysis [*Stoer and Bulirsch*, 1980].

To understand the smallest sample size required in this design, let us consider, for example, the case in which the aliasing-free identity (5) is required to hold in the triangular region $\mathcal{T}_L := \{(l,m): |m| \le l, 0 \le l \le L\}$. Corresponding to this region, there are $2(L+1)^2$ real-valued equations determined by the real and imaginary parts of (5) for an arbitrary (possibly complex-valued) field. It is therefore necessary that the network consist of $J \ge (2(L+1)^2+1)/3$ stations so that the number of free parameters in the network (which is $3J-1$) matches the number of equations (which equals $2(L+1)^2$).

In most numerical simulation schemes for climate modeling it is often desirable that the network be symmetric, so that (1) the stations corresponding to the four combinations of ϕ_j and $-\phi_j$ with θ_j and $\theta_j - \pi$ (mod 2π) all belong to the network, and (2) the stations $\boldsymbol{n}_j$ and $-\boldsymbol{n}_j$, which belong to the network according to point 1, have the same weights. Because of this restriction the number of free parameters reduces to J (instead of $3J-1$), and thus $J \ge 2(L+1)^2$ becomes the minimum requirement for (5) to hold in $\mathcal{T}_L$. For a real-valued field the requirement is $J \ge (L+1)^2$, because the T_{lm} (and the $\hat{T}_{lm}$) are symmetric in the sense that $T^*_{lm} = (-1)^m T_{l,-m}$, so that the number of equations can be reduced by one half. This requirement is consistent with the sampling theorems of *Li and North* [1996].

2.2. Aliased Power

For a given sampling network with the observing stations located at $\boldsymbol{n}_j$, the mean square error (MSE) of the estimator $\hat{T}_{lm}$ for estimating T_{lm} is defined by

$$\epsilon^2_{lm} = \langle |\hat{T}_{lm} - T_{lm}|^2 \rangle,$$

where the angle brackets stand for ensemble average. To evaluate the MSE, we note that $\hat{T}_{lm}$ in (3) can be rewritten as

$$\begin{aligned}\hat{T}_{lm} &= \sum_{j=1}^{J} w_j \sum_{l'=0}^{\infty} \sum_{m'=-l'}^{l'} T_{l'm'}\, Y_{l'm'}(\boldsymbol{n}_j)\, Y^*_{lm}(\boldsymbol{n}_j) \\ &= \sum_{l'=0}^{\infty} \sum_{m'=-l'}^{l'} T_{l'm'}\, \Gamma(l,m,l',m'),\end{aligned} \tag{6}$$

where

$$\Gamma(l,m,l',m') = \sum_{j=1}^{J} w_j\, Y_{l'm'}(\boldsymbol{n}_j)\, Y^*_{lm}(\boldsymbol{n}_j). \tag{7}$$

For any given (l,m) we call $\Gamma(l,m,l',m')$ the aliasing coefficient associated with the spherical harmonic $Y_{l'm'}(\boldsymbol{n})$. Clearly, the structure of $\Gamma(l,m,l',m')$ shows how the aliasing effect from different spherical harmonics occurs in the estimator $\hat{T}_{lm}$.

For a homogeneous random field $T(\boldsymbol{n})$ with $\langle T(\boldsymbol{n})\rangle = 0$, let $\rho(x)$, with $\rho(1) = 1$, be the correlation function of $T(\boldsymbol{n})$ as defined by

$$\langle T(\boldsymbol{n})\, T(\boldsymbol{n}')\rangle = \sigma^2 \rho(\boldsymbol{n}\cdot\boldsymbol{n}'),$$

where $\sigma^2 = \langle T^2(\boldsymbol{n})\rangle$ is the variance (or power) of $T(\boldsymbol{n})$. The power spectrum of $T(\boldsymbol{n})$ is defined as

$$\rho_l = \frac{1}{2}\int_{-1}^{1} \rho(x)\, P_l(x)\, dx \qquad (l = 0,1,2,\cdots),$$

where $P_l(x)$ represents the Legendre polynomial of degree l. It can be shown that

$$\rho(x) = \sum_{l=0}^{\infty} (2l+1)\, \rho_l\, P_l(x). \tag{8}$$

Because the field $T(\boldsymbol{n})$ is homogeneous, different spherical harmonic coefficients are uncorrelated. In fact, one can write [*Li and North*, 1996]

$$\langle T_{lm} T^*_{l'm'}\rangle = 4\pi\sigma^2 \rho_l\, \delta_{l'-l}\, \delta_{m'-m}, \tag{9}$$

where δ_k is the Kronecker delta with $\delta_0 = 1$ and $\delta_k = 0$ if $k \neq 0$.

Using these results, one can derive the following formula for the MSE:

$$\epsilon^2_{lm} = 4\pi\sigma^2 \Bigg\{ \rho_l\, [1 - \Gamma(l,m,l,m)]^2 + \sum_{(l',m')\neq(l,m)} \rho_{l'}\, \Gamma^2(l,m,l',m') \Bigg\}. \tag{10}$$

Note that, according to (9), the power (or variance) of $T_{l'm'}$ is $\langle |T_{l'm'}|^2\rangle = 4\pi\sigma^2\rho_{l'}$. Therefore the relationship given by (10) reveals that the MSE ϵ^2_{lm} is composed of aliased powers from all spherical harmonic components via a weighted sum. For this reason we also refer to ϵ^2_{lm} as the (total) aliased power in the estimator $\hat{T}_{lm}$.

To measure the strength of the aliasing effect in $\hat{T}_{lm}$ relative to the power of T_{lm}, one may define the (total) relative aliased power in $\hat{T}_{lm}$ as

$$e^2_{lm} = \frac{\epsilon^2_{lm}}{\langle |T_{lm}|^2\rangle} = [1 - \Gamma(l,m,l,m)]^2 + \sum_{(l',m')\neq(l,m)} \frac{\rho_{l'}}{\rho_l}\, \Gamma^2(l,m,l',m'). \tag{11}$$

Clearly, in (11) the proportion of the total aliased power that can be attributed to the $2l'+1$ spherical harmonics of degree l' (i.e., $Y_{l'm'}(\boldsymbol{n})$ with $m' = 0, \pm1, \cdots, \pm l'$) is given by

$$d_{lm}(l') = \frac{1}{e^2_{lm}} \Bigg\{ [1 - \Gamma(l,m,l,m)]^2\, \delta_{l'-l} + \frac{\rho_{l'}}{\rho_l} \sum_{m'=-l'}^{l'} \Gamma^2(l,m,l',m')\, (1 - \delta_{l'-l}\delta_{m'-m}) \Bigg\}. \tag{12}$$

Since $\sum_{l'=0}^{\infty} d_{lm}(l') = 1$, we call $d_{lm}(l')$ the (normalized) spectral density of aliased power of the estimator $\hat{T}_{lm}$. It is clear that $d_{lm}(l')$ describes the distribution of the aliased power over different wave numbers of the spherical harmonics.

If the network is designed so that $\hat{T}_{lm} = T_{lm}$ when $T(\boldsymbol{n}) = Y_{lm}(\boldsymbol{n})$, then, according to (6), the identity

$$\Gamma(l,m,l,m) = \sum_{j=1}^{J} w_j\, |Y_{lm}(\boldsymbol{n}_j)|^2 = 1 \tag{13}$$

must be satisfied. (Note that $T(\boldsymbol{n}) = Y_{lm}(\boldsymbol{n})$ implies $T_{l'm'} = \delta_{l'-l}\,\delta_{m'-m}$.) We call (13) the unbiasedness condition. Clearly, the unbiasedness condition (13) reduces to the normalization condition (4) if $l = m = 0$. When (13) is satisfied, the leading terms vanish in (10)–(12), because $[1 - \Gamma(l,m,l,m)]^2 = 0$.

3. Gauss-Legendre Networks

For computational simplicity, one often needs a network that treats the longitude and latitude locations separately, so that $\boldsymbol{n}_j$ takes the form

$$\boldsymbol{n}_{pq} = (\cos\phi_q \cos\theta_p, \cos\phi_q \sin\theta_p, \sin\phi_q).$$

The Gauss-Legendre (GL) networks [e.g., *Washington and Parkinson*, 1986; *Li and North*, 1996] are such examples. A GL network of size $J = MN$ can be obtained as follows: (1) Place the stations at the intersections of M latitude rings and N longitude rings, where the latitudes θ_p are uniformly spaced and the latitudes ϕ_q are determined by the zeros of the Legendre polynomial $P_N(\sin\phi)$. (2) Determine the weights according to $w_{pq} = (2\pi/M)g_q$, where the g_q are defined by

$$g_q = \int_{-1}^{1} \prod_{j=1,\, j\neq q}^{N} \frac{x - x_j}{x_q - x_j}\, dx$$

with $x_q = \sin\phi_q$ being the zeros of $P_N(x)$. It is easy to see that a GL network is symmetric in the sense discussed in section 2.

Let $P_{lm}(x)$ be the associated Legendre functions defined by [*Arfken*, 1985]

$$P_{lm}(x) = (-1)^m (1-x^2)^{m/2} \frac{d^m}{dx^m} P_l(x).$$

Then the spherical harmonics $Y_{lm}(\boldsymbol{n})$ can be written as

$$Y_{lm}(\boldsymbol{n}) = C_{lm}\, P_{lm}(\sin\phi)\, e^{im\theta},$$

where

$$C_{lm} = (-1)^m \sqrt{\frac{2l+1}{4\pi}\frac{(l-m)!}{(l+m)!}}.$$

Therefore, for a GL network, one obtains

$$\Gamma(l,m,l,m) = 2\pi C_{lm}^2 \sum_{q=1}^{N} g_q\, P_{lm}^2(\sin\phi_q). \tag{14}$$

Since $P_{lm}^2(x)$ is a polynomial of degree $2l$, one can apply the Gaussian quadrature formula to (14) and obtain

$$\begin{aligned}\Gamma(l,m,l,m) &= 2\pi C_{lm}^2 \int_{-1}^{1} P_{lm}^2(x)\, dx \\ &= 1 \quad \forall\, (l,m) \in \mathcal{T}_{N-1}. \end{aligned}\tag{15}$$

In other words, an $M \times N$ GL network satisfies the unbiasedness condition (13) in $\mathcal{T}_{N-1}$. This condition, however, cannot be extended to higher order terms. For instance, if $l = N$ and $m = 0$, we have $P_{lm}(\sin\phi_q) = P_N(x_q) \equiv 0$, so that $\Gamma(N,0,N,0) = 0 \neq 1$. In this sense the GL networks are only partially unbiased.

When N is very small, the distribution of the stations in a GL network is highly nonuniform in the north-south direction. When N becomes large, the distribution gradually approaches uniformity, but because of the spherical geometry the weights w_{pq} decrease with respect to the latitude ϕ_q and are highly nonuniform with respect to q.

4. Aliased Power in GL Networks

In this section we investigate the composition of the aliased power ϵ_{lm}^2 when the estimator $\hat{T}_{lm}$ is obtained from the GL networks. Since the power spectrum ρ_l of the field $T(\boldsymbol{n})$ can either be derived from a physical model or estimated from data (see section 5), the major task here is to evaluate the aliasing coefficients $\Gamma(l,m,l',m')$.

To evaluate $\Gamma(l,m,l',m')$, we note that for the GL networks, equation (7) becomes

$$\begin{aligned}&\Gamma(l,m,l',m') \\ &\quad= \sum_{p=1}^{M}\sum_{q=1}^{N} \frac{2\pi}{M}\, g_q\, Y_{l'm'}(\boldsymbol{n}_{pq})\, Y_{lm}^*(\boldsymbol{n}_{pq}) \\ &\quad= C_{lm}C_{l'm'}\, A_M(m,m')\, B_N(l,m,l',m'),\end{aligned}\tag{16}$$

where

$$A_M(m,m') = \frac{2\pi}{M}\sum_{p=1}^{M} e^{i(m'-m)(-\pi+2\pi p/M)},$$

$$B_N(l,m,l',m') = \sum_{q=1}^{N} g_q\, P_{lm}(\sin\phi_q)\, P_{l'm'}(\sin\phi_q).$$

It is straightforward to show that

$$A_M(m,m') = 2\pi \sum_{s=-\infty}^{\infty} (-1)^{Ms}\delta_{m'-(m+Ms)}. \tag{17}$$

Combining this with (6) and (16) leads to the conclusion that $T_{l'm'}$ may contribute to the aliasing error in $\hat{T}_{lm}$ only if $m' = m + Ms$ for some integer s. Furthermore, since $P_{lm}(-x) = (-1)^{l+m}P_{lm}(x)$, we have $P_{lm}(-x)\, P_{l'm'}(-x) = (-1)^{l+l'+Ms}P_{lm}(x)\, P_{l'm'}(x)$ for $m' = m + Ms$. Also note that the x_q are symmetrically distributed around zero and that if $x_{q'}$ is the mirror of x_q (i.e., $x_{q'} = -x_q$), then both of them get the same weight $g_{q'} = g_q$. Therefore, if l' makes $l + l' + Ms$ an odd number, then $P_{lm}(x)\, P_{l'm'}(x)$ is an odd function of x, and

$$B_N(l,m,l',m') = \sum_{q=1}^{N} g_q\, P_{lm}(x_q)\, P_{l'm'}(x_q) = 0.$$

This result, combined with (6), (16), and (17), implies that $T_{l'm'}$ is aliased to T_{lm} only if (l',m') takes the form $(l + Ms + 2r, m + Ms)$ for some integers r and s.

By common practice in GCM modeling we always assume that M is an even integer in the sequel. Under this assumption the spherical harmonic components that may contribute to the aliasing error in $\hat{T}_{lm}$ are characterized by (l',m') being of the form $(l+2r, m+Ms)$, where r and s are integers satisfying $-l/2 \leq r < \infty$ and $-(l+2r+m)/M \leq s \leq (l+2r-m)/M$, or $-\infty < s < \infty$ and $(|m+Ms|-l)/2 \leq r < \infty$. Let the domain of (r,s) defined by these inequalities be denoted by $\mathcal{A}_{lm}$. Then we can express $\hat{T}_{lm}$ as

$$\hat{T}_{lm} = \sum_{(r,s)\in\mathcal{A}_{lm}} T_{l+2r,m+Ms}\, \Gamma(l,m,l+2r,m+Ms). \tag{18}$$

Since $(0,0) \in \mathcal{A}_{lm}$, the term $T_{lm}\,\Gamma(l,m,l,m)$ always appears on the right-hand side of (18). For $(l,m) \in \mathcal{T}_{N-1}$ we have $\Gamma(l,m,l,m) = 1$ due to the unbiasedness condition (15) satisfied by the GL networks.

Furthermore, the GL design also ensures that [*Li and North*, 1996]

$$\begin{aligned}&\Gamma(l,m,l+2r,m) = 0 \\ &\qquad \forall\ -l/2 \leq r < N-l, r \neq 0.\end{aligned}\tag{19}$$

Therefore, with $(l',m') = (l+2r, m+Ms)$, if $T_{l'm'}$ is an alias of T_{lm} and $s \neq 0$, then the distance between $T_{l'm'}$ and T_{lm} in the spectral (wave number) domain, i.e.,

$$\mu = \sqrt{(l'-l)^2 + (m'-m)^2},$$

satisfies $\mu = \sqrt{(2r)^2 + (Ms)^2} \geq M$; if $s = 0$, then the distance satisfies $\mu = 2r \geq 2(N-l)$ as long as $N > l$. In other words, the aliases of T_{lm} in an $M \times N$ GL network are separated in the spectral domain by a distance of at least M if the zonal wave numbers of the aliases are different from the zonal wave number of T_{lm}, or by a distance of least $2(N-l)$ if the aliases and T_{lm} have

the same zonal wave number but different degrees (for $N > l$).

To visualize the structure of the aliasing coefficients $\Gamma(l,m,l',m')$ for the GL networks, we present two examples in Figure 1 that demonstrate how the $T_{l'm'}$ are aliased to T_{00} in the estimator $\hat{T}_{00}$. In this figure the small squares represent the aliasing coefficients that are annihilated by the GL design but may be eliminated in general by other symmetric networks. For $\hat{T}_{00}$ the annihilated coefficients correspond to $m' = 0$ and $l' = 2, 4, \cdots, 2(N-1)$. Also note that the sparseness of nonzero aliasing coefficients increases as the number of stations is increased, resulting in a decrease of the aliasing effect. Similar behavior is found in the estimators of other spherical harmonic coefficients, as supported by two additional examples in Figure 2.

If the field is band limited in the sense that $T_{lm} = 0$ whenever $l > L_0$, then the Gaussian sampling theorem ensures that with the choice of $N \geq M/2 > L_0$ one obtains $\epsilon^2_{lm} = 0$ and therefore $\hat{T}_{lm} = T_{lm}$ for any $(l,m) \in \mathcal{T}_{L_0}$ [*Li and North*, 1996]. Because the band-limited field can be perfectly reconstructed from T_{lm} with $(l,m) \in \mathcal{T}_{L_0}$ [*Li and North*, 1996], the GL network can completely eliminate the aliasing error if the stations are sufficient. The GL network is also efficient because it achieves the aliasing-free identity in $\mathcal{T}_{L_0}$ with the minimal number of stations, $J_0 = 2(L_0+1)^2$, required under the symmetry condition.

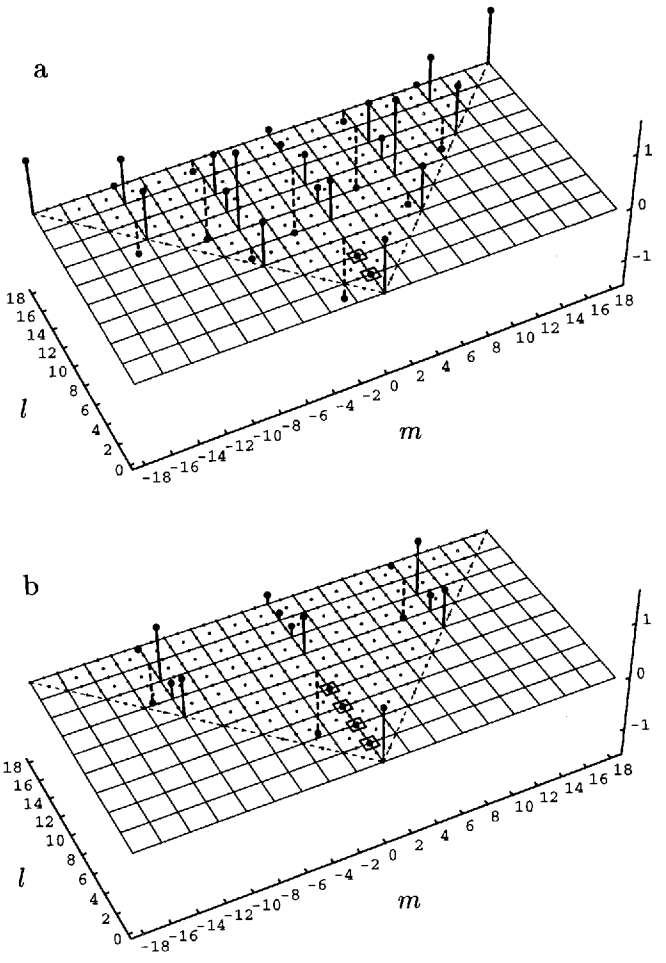

Figure 1. Aliasing coefficients $\Gamma(0,0,l,m)$ in the estimator $\hat{T}_{00}$ using GL networks. (a) An 18-station network with $N = \frac{1}{2}M = 3$; (b) A 50-station network with $N = \frac{1}{2}M = 5$. The solid and dashed arrows stand for positive and negative coefficients, respectively. The arrows at $(l,m) = (0,0)$ define the unit length. The triangular arrays of dots indicate the domain of aliasing coefficients. The small squares indicate zero aliasing coefficients achieved by the GL design but in general cannot be achieved by other symmetric networks.

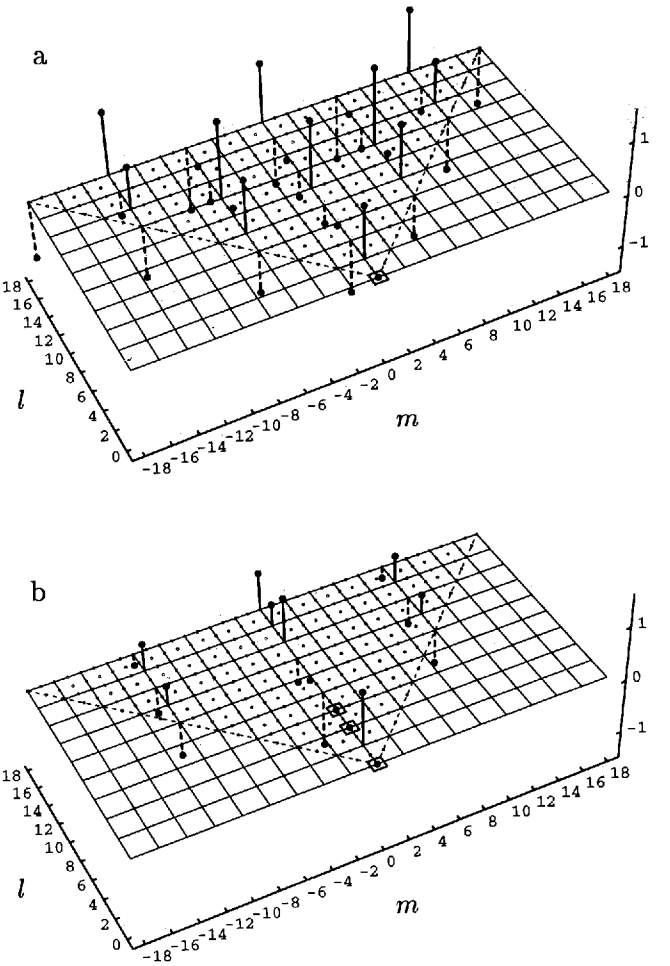

Figure 2. Aliasing coefficients $\Gamma(2,0,l,m)$ in $\hat{T}_{20}$ using GL networks. (a) An 18-station network ($N = \frac{1}{2}M = 3$); (b) A 50-station network ($N = \frac{1}{2}M = 5$). The arrows at $(l,m) = (2,0)$ define the unit length. (See Figure 1 caption for more details.)

Because the special structure of $\Gamma(l,m,l',m')$ in the GL networks it is easy to show from (18) that the aliased power ϵ^2_{lm} for a homogeneous field takes the form

$$\epsilon^2_{lm} = 4\pi\sigma^2 \Bigg\{ \rho_l \left[1 - \Gamma(l,m,l,m)\right]^2 + \sum_{(r,s)\in\mathcal{A}^0_{lm}} \rho_{l+2r}\, \Gamma^2(l,m,l+2r,m+Ms) \Bigg\}, \tag{20}$$

where $\mathcal{A}_{lm}^0 = \mathcal{A}_{lm} \setminus (0,0)$. Similarly, we can express the relative aliased power e_{lm}^2 as

$$e_{lm}^2 = [1 - \Gamma(l,m,l,m)]^2 + \sum_{(r,s)\in\mathcal{A}_{lm}^0} \frac{\rho_{l+2r}}{\rho_l} \Gamma^2(l,m,l+2r,m+Ms). \tag{21}$$

Note that $[1 - \Gamma(l,m,l,m)]^2 = 0$ if $(l,m) \in \mathcal{T}_{N-1}$, because the GL networks are unbiased in $\mathcal{T}_{N-1}$. Also note that the identity (19) holds for the GL networks.

To end this section, we point out that (20) and (21) also hold for networks in which the latitude rings are uniformly spaced but the latitude rings are not necessarily located at the zeros of a Legendre polynomial. An example of such networks is one that places the latitude rings uniformly with equal weights so that $\phi_q = -\pi/2 + \pi q/(N+1)$ and $g_q = 2/N$ for $q = 1, \cdots, N$. We call this network a latitude-longitude uniform (LLU) network. The LLU networks are symmetric but (19) may not hold in general.

5. Noise-Forced Energy Balance Model

In this section we consider a homogeneous field generated by a simple climate model. To be more specific, consider the white noise forced linear energy balance model given by

$$\tau_0 \frac{\partial}{\partial t} T(\boldsymbol{n},t) - \lambda_0^2 \nabla^2 T(\boldsymbol{n},t) + T(\boldsymbol{n},t) = F(\boldsymbol{n},t), \tag{22}$$

where $T(\boldsymbol{n},t)$ is the local departure of the temperature from its climatology, τ_0 is an inherent timescale, and λ_0 is an inherent length scale. As we mentioned in the introduction, this paper only concerns the low-frequency limit of the climate process. For this purpose the time-dependent term in (22) is not crucial and can be omitted. The resulting time-independent EBM becomes

$$-\lambda_0^2 \nabla^2 T(\boldsymbol{n}) + T(\boldsymbol{n}) = F(\boldsymbol{n}), \tag{23}$$

where λ_0 is the length scale in units of the Earth radius and $F(\boldsymbol{n})$ is the spherical white noise field satisfying $\langle F(\boldsymbol{n})F(\boldsymbol{n}')\rangle = \sigma_F^2 \delta(\boldsymbol{n} - \boldsymbol{n}')$ with $\delta(\cdot)$ being the Dirac delta. Let the spherical harmonic expansion of $F(\boldsymbol{n})$ be

$$F(\boldsymbol{n}) = \sum_{l=0}^{\infty} \sum_{m=-l}^{l} F_{lm} Y_{lm}(\boldsymbol{n}), \tag{24}$$

where $F_{lm} = \int F(\boldsymbol{n}) Y_{lm}^*(\boldsymbol{n})\, d\Omega$. Then, by substituting (1) and (24) into (23), we obtain

$$T_{lm} = \frac{F_{lm}}{1 + \lambda_0^2 l(l+1)}. \tag{25}$$

Since $\langle |F_{lm}|^2 \rangle = 4\pi\sigma_F^2$, it follows that

$$4\pi\sigma^2 \rho_l = \langle |T_{lm}|^2 \rangle = \frac{4\pi\sigma_F^2}{(1 + \lambda_0^2 l(l+1))^2}.$$

Therefore, with $\rho_0 = \sigma_F^2/\sigma^2$, we can write

$$\rho_l = \frac{\rho_0}{(1 + \lambda_0^2 l(l+1))^2} \quad (l = 0, 1, \cdots). \tag{26}$$

Note that $\rho_l = O(l^{-4})$ as $l \to \infty$. In other words, the power spectrum ρ_l of the field decays as fast as l^{-4} with respect to the degree l. Using the condition $\rho(1) = 1$ and (8), one can determine ρ_0 from the identity

$$\sum_{l=0}^{\infty} (2l+1) \frac{\rho_0}{(1 + \lambda_0^2 l(l+1))^2} P_l(1) = 1.$$

In fact, since $P_l(1) = 1$ for all l, one obtains

$$\rho_0 = \left\{ \sum_{l=0}^{\infty} \frac{2l+1}{(1 + \lambda_0^2 l(l+1))^2} \right\}^{-1}.$$

Note that ρ_0 is a monotone increasing function of λ_0 as shown in Figure 3a. In our examples, the value of λ_0

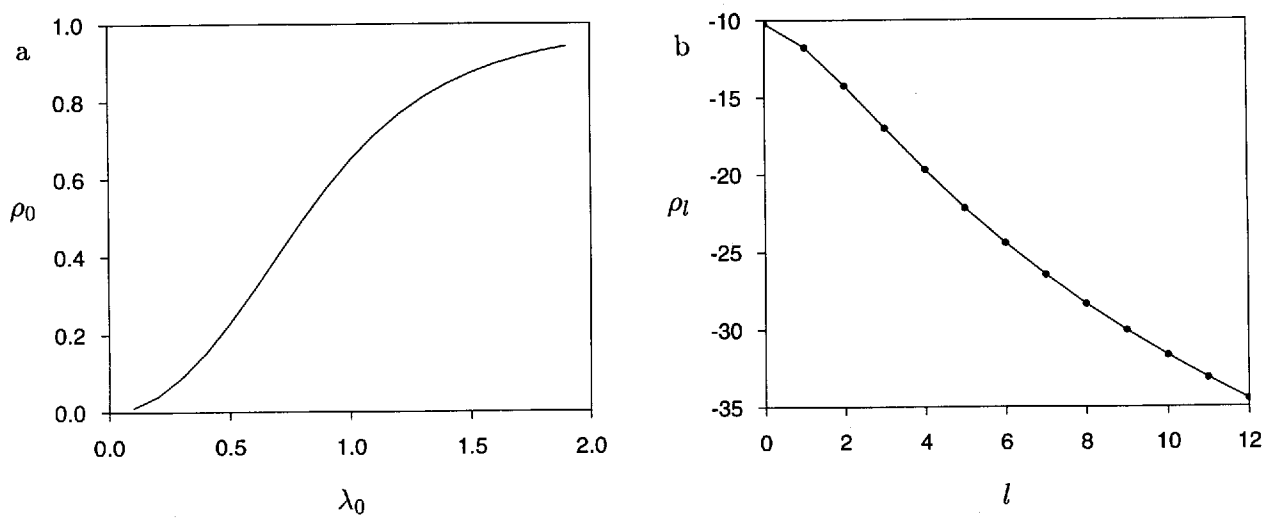

Figure 3. (a) Plot of ρ_0 as a function of λ_0 for the white noise driven time-independent EBM. (b) The EBM-based power spectrum ρ_l (in decibels) as a function of the degree l ($\lambda_0 = 0.3141$).

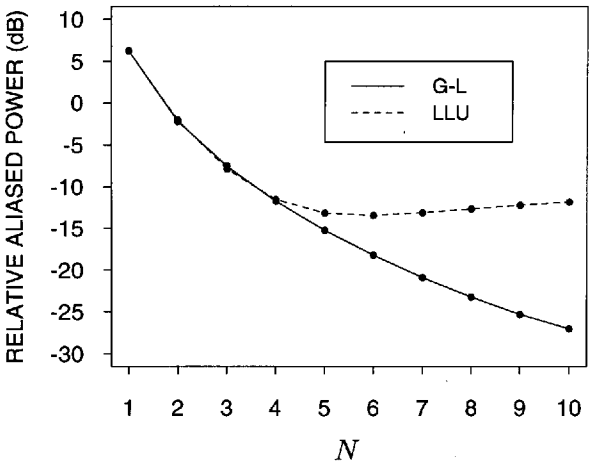

Figure 4. Plot of the relative aliased power e_{00}^2 (in decibels) as a function of $N = \frac{1}{2}M$ for the white noise driven EBM.

is determined by the length scale of the anomaly field. For the annual mean field the EBM length scale is about 2000 km [*Kim and North*, 1993]. If we take the radius of the Earth to be 6367 km, then λ_0 becomes $2000/6367 = 0.3141$, and the corresponding ρ_0 is 0.0954. With this value the EBM spectrum ρ_l is shown in Figure 3b. In the sequel we always use $\lambda_0 = 0.3141$ in the EBM (23).

Using (8) and the fact that $\rho(1) = P_l(1) = 1$, one can also write

$$\sigma^2 = \sum_{l=0}^{\infty} (2l+1)\,\sigma^2 \rho_l. \tag{27}$$

In this expression the total variation of $T(\boldsymbol{n})$ is decomposed into a weighted sum of the power spectrum. Since there are $2l+1$ spherical harmonic components of degree l in the expansion (1), it is evident from (27) that $\rho_l = \langle |T_{lm}|^2 \rangle / (4\pi\sigma^2)$ represents the proportion of variation in $T(\boldsymbol{n})$ that can be attributed to each of the lth-degree harmonics. With this interpretation of the power spectrum one may conclude that the global average T_{00}, which corresponds to the zeroth-degree spherical harmonic $Y_{00}(\boldsymbol{n}) = \sqrt{4\pi}$, describes about 10% of the total variation of the EBM field because $\rho_0 = 0.0954$.

6. Numerical Examples

For the homogeneous field $T(\boldsymbol{n})$ generated by the EBM (23) we estimate the spherical harmonic coefficients T_{lm} by $\hat{T}_{lm}$ in (3), using the observations from a Gauss-Legendre network. In this section we compute the relative aliased power e_{lm}^2 and the spectral density of aliased power $d_{lm}(l')$ and investigate their relationships with the size of the network. The computation was performed by using *Mathematica* 2.2 on a Sun Sparc 10 workstation.

First, consider the estimation of the global average T_{00} by $\hat{T}_{00}$. With $(l,m) = (0,0)$ the formula (20) is simplified as

$$\epsilon_{00}^2 = 4\pi\sigma^2 \sum_{r=1}^{\infty} \rho_{2r} \sum_{s=-\lfloor 2r/M \rfloor}^{\lfloor 2r/M \rfloor} \Gamma^2(0,0,2r,Ms), \tag{28}$$

where $\lfloor \cdot \rfloor$ is the "floor" function such that $\lfloor x \rfloor = n$ if $n \le x < n+1$ for some integer n. Similarly, we obtain

$$e_{00}^2 = \sum_{r=1}^{\infty} \frac{\rho_{2r}}{\rho_0} \sum_{s=-\lfloor 2r/M \rfloor}^{\lfloor 2r/M \rfloor} \Gamma^2(0,0,2r,Ms). \tag{29}$$

Note that in these formulas $\Gamma^2(0,0,2r,Ms) = 0$ if $s = 0$ and $r = 1, \cdots, N-1$.

Using the EBM spectrum (26) and $M = 2N$, Figure 4 and Table 1 show the relationship between the relative aliased power e_{00}^2 in (29) and the network parameter N. In the calculation the infinity sum (29) was replaced by a finite sum over r so that $l' = 2r \le 30$, which, due to (25), is equivalent to assuming that the noise field $F(\boldsymbol{n})$ in the EBM (23) is band limited with $F_{lm} = 0$ for $l > 30$. Note that the size of the network is $J = MN = 2N^2$. It is shown in Figure 4 that with the increase of the number of stations from $J = 2$ ($N = 1$) to $J = 50$ ($N = 5$) the relative aliased power e_{00}^2 decreases approximately from 6 dB to -15 dB, yielding a 21 dB reduction; another 12 dB reduction can be achieved by increasing the number of stations to $J = 200$ ($N = 10$). As is shown in Table 1, the aliased power of the two-station network is more than 4 times as much as the variation of the spherical harmonic coefficient T_{00}, because $e_{00}^2 \doteq 4.2$, whereas the 200-station GL network reduces e_{00}^2 to about 0.002, so that the aliased power in $\hat{T}_{00}$ is only 0.2% of the power of T_{00}.

For comparison, the relative aliased power e_{00}^2 for the uniform design is also presented in Figure 4 and Table 1. As we can see, when the number of stations is small (e.g., $J = 2$–32 or $N = 1$–4), the two designs are almost indistinguishable in terms of the aliasing effect; when

Table 1. Relative Aliased Power e_{00}^2 for Networks of Different Sizes

	Number of Stations ($J = 2N^2$)									
Network	2	8	18	32	50	72	98	128	162	200
Gauss-Legendre	4.2	0.60	0.18	0.067	0.030	0.015	0.008	0.005	0.003	0.002
Latitude-Longitude Uniform	4.2	0.62	0.17	0.071	0.048	0.045	0.049	0.054	0.060	0.066

more stations are employed in the networks, the advantage of the GL design becomes prominent. For example, with 128 stations ($N = 8$) the GL design achieves a 10 dB improvement over the uniform design. Moreover, whereas the aliased power of the GL design decreases as the number of stations grows, the aliased power of the uniform design stops decreasing at $N = 5$; in fact, it starts to increase slightly as N becomes larger. The superior performance of the GL design is primarily due to its effective accommodation of the fact that most of the power of the EBM field $T(\boldsymbol{n})$ comes from the harmonic components of low wave numbers (see Figure 3b).

To investigate the distribution of the aliased power over different wave numbers, we note that for $r = 1, 2, \cdots$, we have $d_{00}(2r-1) = d_{00}(0) = 0$ and

$$d_{00}(2r) = \frac{1}{e_{00}^2}\frac{\rho_{2r}}{\rho_0}\sum_{s=-\lfloor 2r/M\rfloor}^{\lfloor 2r/M\rfloor}\Gamma^2(0,0,2r,Ms). \quad (30)$$

Since the GL design satisfies (19), it is easy to see that with $M = 2N$ we have $d_{00}(2r) = 0$ for $r = 1, \cdots, N-1$.

Using (30), we calculated the $d_{00}(l)$ for two GL networks, one with $N = 2$ ($J = 8$) and the other with $N = 5$ ($J = 50$). The results are shown in Figure 5, where the circles represent the aliased power components that vanish in the GL design but may not vanish in general, and the cross indicates the degree $l = 0$ in question; the aliased power at this point equals zero because the unbiasedness condition (15) is satisfied. As can be seen from Figure 5, the aliased power concentrates on low degrees when the number of stations is small, whereas the concentration shifts to higher degrees when the number of stations is increased; the aliased power components in e_{00}^2 of degree l lower than $2N$ are all annihilated by the GL network of $J = 2N^2$ stations [*Li and North*, 1996].

Similar analysis can be performed for the estimator $\hat{T}_{lm}$. In fact, for any (l, m) the relative aliased power e_{lm}^2 in (21) can be calculated according to the formula

$$e_{lm}^2 = [1-\Gamma(l,m,l,m)]^2 + \sum_{r=-\lfloor l/2\rfloor}^{\infty}\frac{\rho_{l+2r}}{\rho_l} \times \sum_{s=-\lfloor (l+2r+m)/M\rfloor}^{\lfloor (l+2r-m)/M\rfloor}\Gamma^2(l,m,l+2r,m+Ms) \times (1-\delta_s\delta_r). \quad (31)$$

With $r \geq -\lfloor l/2\rfloor$ it can be shown that

$$d_{lm}(l+2r+1) = 0,$$

$$d_{lm}(l) = \frac{1}{e_{lm}^2}\left\{[1-\Gamma(l,m,l,m)]^2 + \sum_{s=-\lfloor (l+m)/M\rfloor}^{\lfloor (l-m)/M\rfloor}\Gamma^2(l,m,l,m+Ms)(1-\delta_s)\right\}, \quad (32)$$

and, for $r \neq 0$,

$$d_{lm}(l+2r) = \frac{1}{e_{lm}^2}\frac{\rho_{l+2r}}{\rho_l}\sum_{s=-\lfloor (l+2r+m)/M\rfloor}^{\lfloor (l+2r-m)/M\rfloor}\Gamma^2(l,m,l+2r,m+Ms). \quad (33)$$

Since $M = 2N$, it is easy to see that $\lfloor (l+2r+m)/M\rfloor = \lfloor (l+2r-m)/M\rfloor = 0$ if $-l/2 \leq r < N-l$. Therefore, for the GL networks, (19) implies that $d_{lm}(l+2r) = 0$ if $r \in \{-\lfloor l/2\rfloor, -\lfloor l/2\rfloor + 1, \cdots, N-l-1\} \setminus \{0\}$. In other words, the GL design eliminates all the aliased power components in e_{lm}^2 whose degrees l' are lower than $2N-l$ but different from l. Moreover, the condition (15) implies that $d_{lm}(l) = 0$ if $l \leq N-1$.

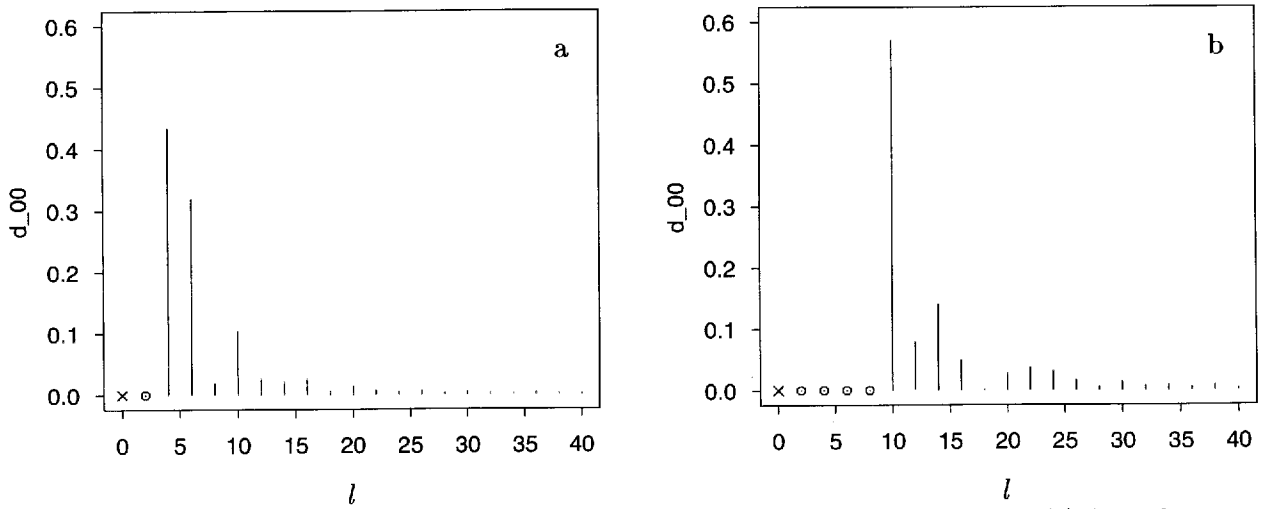

Figure 5. Spectral density of aliased power $d_{00}(l)$ for the white noise driven EBM. (a) An eight-station GL network ($N = \frac{1}{2}M = 2$) with $e_{00}^2 \doteq 0.60$. (b) A 50-station GL network ($N = \frac{1}{2}M = 5$) with $e_{00}^2 \doteq 0.03$.

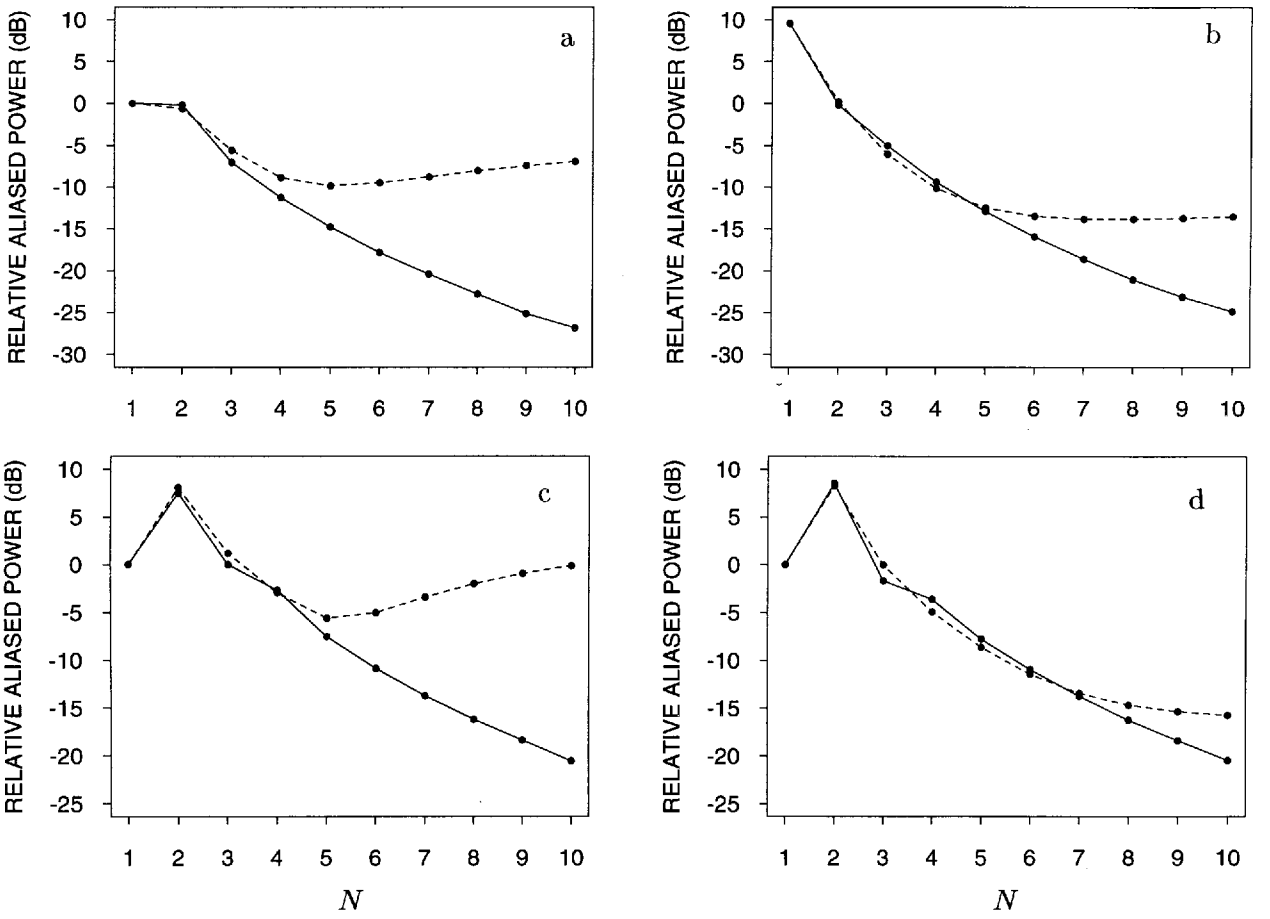

Figure 6. Plot of the relative aliased power e_{lm}^2 (in decibels) as a function of $N = \frac{1}{2}M$ for the white noise driven EBM—solid lines for GL networks and dashed lines for LLU networks. (a) $(l, m) = (1, 0)$; (b) $(l, m) = (1, 1)$; (c) $(l, m) = (3, 0)$; and (d) $(l, m) = (3, 2)$.

In Figure 6 we plot the relative aliased power e_{lm}^2 as a function of $N = M/2$ for several values of (l, m). The calculation was carried out for the GL and LLU networks under the EBM (23). Again, the infinite sum over r in (31) was truncated so that $l' = l + 2r \leq 30$. Observe that in all these cases the GL design eventually outperforms the uniform design as the number of stations becomes sufficiently large. For a fixed number of stations the advantage of the GL networks seems more pronounced for estimating low wave number components ($\mu = \sqrt{l^2 + m^2}$ small) than for estimating high wave number components (μ large). If the stations are insufficient (i.e., N is small), the uniform design may have a small edge (if any) over the GL design. This finding is not surprising, because the EBM power spectrum is not band limited, and even for a band-limited field it is still required that N be greater than the bandwidth in order for the GL design to eliminate the aliasing error [*Li and North*, 1996].

More computational results are given in Tables 2–5, where the e_{lm}^2 in Tables 2 and 3 are calculated by using (31) with the truncation $l' = l + 2r \leq 40$ and the e_{lm}^2 in

Table 2. Relative Aliased Power e_{lm}^2 for 98-Station Networks ($N = \frac{1}{2}M = 7$)

	Gauss-Legendre Network					Latitude-Longitude Uniform Network				
m	$l = 1$	$l = 2$	$l = 3$	$l = 4$	$l = 5$	$l = 1$	$l = 2$	$l = 3$	$l = 4$	$l = 5$
0	0.009	0.021	0.045	0.099	0.22	0.134	0.379	0.461	0.330	0.30
1	0.016	0.021	0.042	0.092	0.20	0.042	0.057	0.287	0.679	1.22
2		0.029	0.045	0.087	0.17		0.059	0.048	0.142	0.34
3			0.061	0.096	0.17			0.082	0.082	0.16
4				0.131	0.20				0.124	0.15
5					0.28					0.21

The infinite series of r in (31) was truncated so that $l' = l + 2r \leq 40$.

Table 3. Relative Aliased Power e_{lm}^2 for 128-Station Networks ($N = \frac{1}{2}M = 8$)

	Gauss-Legendre Network					Latitude-Longitude Uniform Network				
m	$l=1$	$l=2$	$l=3$	$l=4$	$l=5$	$l=1$	$l=2$	$l=3$	$l=4$	$l=5$
0	0.006	0.012	0.026	0.055	0.12	0.157	0.462	0.634	0.542	0.30
1	0.009	0.012	0.025	0.051	0.11	0.042	0.047	0.257	0.615	1.11
2		0.017	0.026	0.050	0.10		0.057	0.036	0.111	0.26
3			0.035	0.055	0.10			0.073	0.059	0.11
4				0.073	0.11				0.098	0.10
5					0.15					0.14

See Table 2 for remarks.

Tables 4 and 5 are based on the truncation $l' = l + 2r \leq 30$. A lower-order truncation is used in Tables 4 and 5 because of the computational difficulties encountered in *Mathematica* for evaluating the associated Legendre functions $P_{lm}(x)$ when (l, m) is too high and $|x|$ is too close to unity (which happens if N is large).

To demonstrate the distribution of the aliased powers given by (32) and (33), we present, as an example, the spectral density of aliased power $d_{11}(l')$ in Figure 7 for the GL and LLU networks of the same size. The calculation shows that the total relative aliased power e_{11}^2 of the GL network is only one third that of the LLU network (0.014 versus 0.042). Figure 7 also shows that for the LLU network nearly 80% of its aliased power can be attributed to the low wave number components with $l' = 1$ and $l' = 3$, whereas the GL design eliminates all aliasing errors from the low wave number components with $l' \leq 2N - l - 1 = 12$. This comparison again suggests that the annihilation of the low wave number components (represented by circles in Figure 7), where most of the energy of the field concentrates, be primarily responsible for the smaller aliased power achieved by the GL design.

7. Discussion and Conclusions

In this paper we have investigated the aliased power of the Gauss-Legendre networks in the estimation of the spherical harmonic components of the surface temperature field over the globe. Using the white noise driven EBM, we have calculated the total aliased power and the spectral distribution of the aliased power for both Gauss-Legendre and latitude-longitude uniform networks. Numerical results show that with a sufficient number of stations the Gauss-Legendre network is able to achieve a smaller aliasing error than a latitude-longitude uniform network of the same size; this result is especially true for the estimation of low wave number components. Of course, the aliased power can be further reduced by simultaneously choosing the weights w_j and perhaps the locations $\boldsymbol{n}_j$ in the network so as to minimize the aliased power [e.g., *Hardin and Upson*, 1993; *Shen et al.*, 1996]. The resulting "optimal" network, however, usually depends on knowledge of the power spectrum of the field. On the other hand, the Gauss-Legendre design, though suboptimal, does not depend on the power spectrum and is particularly effective for a spherical field whose spectrum is band limited [*Li and North*, 1996] or decreases sufficiently rapidly with respect to the wave numbers.

Although the Gauss-Legendre and latitude-longitude uniform networks are particular, we consider them in this paper because they make the analytical investigation more transparent, and the results concerning their properties provide some mathematical insights and theoretical background for further investigations of more realistic networks. The extension of the developed methodology to more realistic networks (e.g., ran-

Table 4. Relative Aliased Power e_{lm}^2 for 162-Station Networks ($N = \frac{1}{2}M = 9$)

	Gauss-Legendre Network					Latitude-Longitude Uniform Network				
m	$l=1$	$l=2$	$l=3$	$l=4$	$l=5$	$l=1$	$l=2$	$l=3$	$l=4$	$l=5$
0	0.003	0.007	0.015	0.030	0.062	0.180	0.540	0.810	0.813	0.532
1	0.005	0.007	0.013	0.028	0.058	0.043	0.040	0.235	0.572	1.036
2		0.010	0.015	0.026	0.052		0.057	0.029	0.088	0.212
3			0.020	0.030	0.054			0.070	0.046	0.074
4				0.040	0.061				0.084	0.071
5					0.081					0.109

The infinite series of r in (31) was truncated so that $l' = l + 2r \leq 30$.

Table 5. Relative Aliased Power e_{lm}^2 for 200-Station Networks ($N = \frac{1}{2}M = 10$)

	Gauss-Legendre Network					Latitude-Longitude Uniform Network				
m	$l=1$	$l=2$	$l=3$	$l=4$	$l=5$	$l=1$	$l=2$	$l=3$	$l=4$	$l=5$
0	0.002	0.005	0.009	0.018	0.039	0.202	0.614	0.979	1.103	0.886
1	0.003	0.004	0.009	0.017	0.035	0.045	0.037	0.223	0.545	0.986
2		0.006	0.009	0.017	0.033		0.058	0.027	0.079	0.190
3			0.012	0.019	0.032			0.070	0.041	0.060
4				0.025	0.039				0.081	0.060
5					0.049					0.097

See Table 4 for remarks.

domly distributed stations) will be the major subject of a forthcoming paper.

We should point out that the estimators $\hat{T}_{lm}$ defined by (3) are closely related to the weighted least squares (WLS) estimators [*Trampert and Snieder*, 1996]. Instead of discretizing the integral (2) with the sum (3), the WLS approach fits the data $\{T(\boldsymbol{n}_1), \cdots, T(\boldsymbol{n}_J)\}$ with a finite order (truncated) spherical function

$$\tilde{T}(\boldsymbol{n}) = \sum_{l=0}^{L} \sum_{m=-l}^{l} \tilde{T}_{lm}\, Y_{lm}^*(\boldsymbol{n})$$

whose coefficients $\tilde{T}_{lm}$ are determined by minimizing the weighted sum of squared errors

$$\mathrm{WSSE} = \sum_{j=1}^{J} w_j\, |T(\boldsymbol{n}_j) - \tilde{T}(\boldsymbol{n}_j)|^2.$$

The optimal coefficients $\tilde{T}_{lm}$ are the WLS estimators of T_{lm} for $(l,m) \in \mathcal{T}_L$, and it is easy to show that they satisfy the linear equations

$$\sum_{l'=0}^{L} \sum_{m'=-l'}^{l'} \Gamma(l,m,l',m')\, \tilde{T}_{l'm'} = \hat{T}_{lm} \qquad (34)$$

for $(l,m) \in \mathcal{T}_L$, where the $\hat{T}_{lm}$ are defined by (3) and $\Gamma(l,m,l',m')$ is defined by (7). With an $M \times N$ GL network, such that $M > 2L$ and $N > L$, it follows that $\tilde{T}_{lm} = \hat{T}_{lm}$ for all $(l,m) \in \mathcal{T}_L$, because $\Gamma(l,m,l',m') = \delta_{l-l'}\, \delta_{m-m'}$ for any $(l,m), (l',m') \in \mathcal{T}_L$. This result implies that if the sampling rate is sufficiently high in the GL network, then the estimators $\hat{T}_{lm}$ in (3) coincide with the WLS estimators $\tilde{T}_{lm}$ in the truncated triangular region $\mathcal{T}_L$.

Equation (34) also provides an avenue to the understanding of the aliasing errors in the WLS estimators. For simplicity, let $\tilde{\boldsymbol{t}}$, $\hat{\boldsymbol{t}}$, and $\boldsymbol{t}$ denote the vectors formed in the same way by $\tilde{T}_{lm}$, $\hat{T}_{lm}$, and T_{lm}, respectively, with $(l,m) \in \mathcal{T}_L$, and let $\boldsymbol{\Gamma}$ denote the $(L+1)^2$-by-$(L+1)^2$ coefficient matrix in (34). Then one can rewrite (34) as $\boldsymbol{\Gamma}\tilde{\boldsymbol{t}} = \hat{\boldsymbol{t}}$ so that $\tilde{\boldsymbol{t}} = \boldsymbol{\Gamma}^{-1}\hat{\boldsymbol{t}}$. One can also rewrite (6) as $\hat{\boldsymbol{t}} = \boldsymbol{\Gamma}\boldsymbol{t} + \boldsymbol{r}$, where $\boldsymbol{r}$ is a vector formed in the same way as $\boldsymbol{t}$, with the (l,m)th element being $R_{lm} = \sum_{l'=L+1}^{\infty} \sum_{m'=-l'}^{l'} T_{l'm'}\, \Gamma(l,m,l'm')$ for $(l,m) \in \mathcal{T}_L$. Combining these expressions leads to $\tilde{\boldsymbol{t}} = \boldsymbol{t} + \boldsymbol{\Gamma}^{-1}\boldsymbol{r}$, and therefore the total MSE of the WLS estimators can be easily calculated according to

$$\begin{aligned} \epsilon_{WLS}^2 &= \langle (\tilde{\boldsymbol{t}} - \boldsymbol{t})^H (\tilde{\boldsymbol{t}} - \boldsymbol{t}) \rangle \\ &= \mathrm{tr}\langle (\tilde{\boldsymbol{t}} - \boldsymbol{t})\, (\tilde{\boldsymbol{t}} - \boldsymbol{t})^H \rangle = \mathrm{tr}(\boldsymbol{\Gamma}^{-1} \langle \boldsymbol{r}\, \boldsymbol{r}^H \rangle\, \boldsymbol{\Gamma}^{-H}), \end{aligned}$$

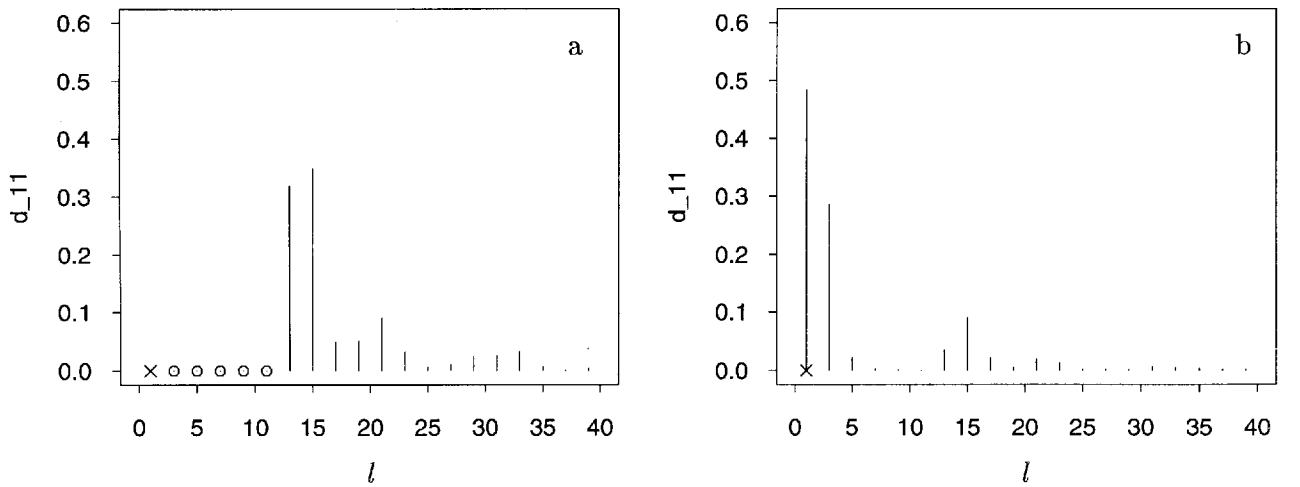

Figure 7. Spectral density of aliased power $d_{11}(l)$ for the white noise driven EBM. (a) A 98-station GL network ($N = \frac{1}{2}M = 7$) with $e_{11}^2 \doteq 0.014$. (b) A 98-station LLU network with $e_{11}^2 \doteq 0.042$.

where tr(·) represents the trace of a matrix and the superscript H stands for Hermitian transpose. Similarly, the total MSE of $\hat{T}_{lm}$ can be written as

$$\epsilon^2 = \sum_{l=0}^{L} \sum_{m=-l}^{l} \epsilon_{lm}^2 = \langle (\hat{\boldsymbol{t}} - \boldsymbol{t})^H (\hat{\boldsymbol{t}} - \boldsymbol{t}) \rangle$$
$$= \mathrm{tr}[(\mathbf{I} - \boldsymbol{\Gamma}) \langle \boldsymbol{t}\,\boldsymbol{t}^H \rangle (\mathbf{I} - \boldsymbol{\Gamma})^H] + \langle \boldsymbol{r}^H \boldsymbol{r} \rangle.$$

For a GL network of size $M \times N$ with $M > 2L$ and $N > L$ one obtains $\boldsymbol{\Gamma} = \mathbf{I}$, so that the total MSEs become $\epsilon^2 = \epsilon_{WLS}^2 = \langle \boldsymbol{r}^H \boldsymbol{r} \rangle = \langle \boldsymbol{r}\,\boldsymbol{r}^H \rangle$. Note that in general the computation of the WLS estimators $\tilde{T}_{lm}$ requires the inversion of the matrix $\boldsymbol{\Gamma}$, which can be burdensome if L is large, whereas the computation of $\hat{T}_{lm}$ is quite straightforward.

Aliased power in spectral GCMs can contaminate the output quite seriously. However, few modelers have paid much attention to the fact that the degree of nonlinearity can also affect the required resolution of the networks for spectral modeling. Here the degree of nonlinearity is defined in the same way as it is in fluid dynamics. For example, the degree of nonlinearity for the Navier-Stokes equations is two. We feel that in order to achieve the aliasing-free transformation the demand on stations increases quadratically with the increase of the degree of nonlinearity. Therefore, when nonlinearity is strong, the spectral modeling approach may have little advantage in practice over the finite difference approach. In particular, if the feedback nonlinearity is present, then the spectral modeling can cause serious problems due to the aliasing effect when the stations are insufficient. This problem deserves further research.

Acknowledgments. The authors would like to thank a referee for bringing the weighted least squares method to their attention. They also gratefully acknowledge the support of a grant from the Department of Energy's CHAMMP program and a grant from the Climate Dynamics program of NSF. S. S. wishes to thank the Environment Canada for a grant from the Atmospheric Environment Service.

References

Arfken, G., *Mathematical Methods for Physics*, 3rd ed., Academic, San Diego, Calif., 1985.

Chen, X., The aliased and the dealiased spectral models of the shallow-water equations, *Mon. Weather Rev., 121*, 834–852, 1993.

Hardin, J. W. and R. B. Upson, Estimation of the global average temperature with optimally weighted point gauges, *J. Geophys. Res., 98*, 23,275–23,282, 1993.

Kim, K.-Y. and G. R North, EOF analysis of surface temperature field in a stochastic climate model, *J. Clim., 6*, 1681–1690, 1993.

Kim, K.-Y., G. R. North, and S. S. Shen, Optimal estimation of spherical harmonic components from a sample with spatially nonuniform covariance statistics, *J. Clim., 9*, 635–645, 1996.

Li, T. H., and G. R. North, Aliasing effects and sampling theorems for spherical random fields when sampled on a finite grid, *Tech. Rep. 247*, Dep. of Stat., Texas A&M Univ., College Station, 1996.

Shen, S. S., G. R. North, and K.-Y. Kim, Spectral approach to optimal estimation of the global average temperature, *J. Clim., 7*, 1999–2007, 1994.

Shen, S. S., G. R. North, and K.-Y. Kim, Optimal estimation of the spherical harmonic components of the surface air temperature, *Environmetrics, 7*, 261–276, 1996.

Stoer, J. and R. Bulirsch, *Introduction to Numerical Analysis*, Springer, New York, 1980.

Trampert, J., and Snieder R., Model estimations biased by truncated expansions: Possible artifacts in seismic tomography, *Science, 271*, 1257–1260, 1996.

Washington, W. M., and C. L. Parkinson, *An Introduction to Three-Dimensional Climate Modeling*, Univ. Sci. Books, Mill Valley, Calif., 1986.

T. H. Li, Department of Statistics, Texas A&M University, College Station, Texas 77843-3143. (e-mail: thl@stat.tamu.edu)

G. R. North, Climate System Research Program, Department of Meteorology, Texas A&M University, College Station, Texas 77843-3150.

S. S. Shen,[1] Center for Climate System Research, University of Tokyo, Tokyo 153, Japan.

(Received May 24, 1996; revised October 11, 1996; accepted October 11, 1996.)